Stress analysis in a classical double lap, adhesively bonded joint with a layerwise model

Alberto Diaz Diaza,, Reda Hadj-Ahmed, Gilles Foret , Alain Ehrlacher

Abstract

This paper focuses on stress analysis in classical double lap, adhesively bonded joints having constant layer thicknesses. Several analytical methods found in the literature do not provide adequate information on stresses at the adherend/adhesive interfaces. In these methods, the adhesive thickness is assumed to be small compared to that of the adherends and the stresses to be uniform through the adhesive thickness. Herein, the model proposed by the authors can be considered as a stacking of Reissner–Mindlin plates (six plates for a double lap joint). The equations based on stacked plates were applied to the geometry of a symmetrical, double- lap, adhesively bonded joint. Finally, the model has been validated by comparing the model results with those of a finite element calculation.

Introduction

Structural designers are interested in the strength evaluation under service conditions. A reliable prediction of stresses at locations where a high risk of crack initiation exists is thus a necessary step in designing mechanical structures. Simplified models [1–5] and solid finite element calculations [6,7] show that in an adhesive joint, both shear and normal stresses reach their maximum value in the vicinity of the bond edges. These stress concentra- tions

often lead to the joint failure. In an adhesive joint, three kinds of failure are possible. The first is adhesive failure, which occurs at the adherend/adhesive interface. The second is cohesive failure, which occurs in the adhesive. The last kind of failure is mixed: it starts out as an adhesive crack and then quickly becomes a cohesive failure.

In the majority of models employed for adhesive joints, stresses are considered constant through the layer thickness [1,8–10]. In addition, the shear stress in the adhesive layer is often taken as a linear function of the difference between the displacement of the outer adherend and the displacement of the inner adherend (see Fig. 1). These models, in classical terms are called shear lag models. Their constitutive equations are detai- led in Appendix A. In order, to correctly estimate the failure in the adhesive layer, a more complex model is needed for calculating the stresses at the adhesive/adherend interfaces.

A more complex model is the layerwise model called M4-5N (multi-particle model of multi-layered materials with five kinematic fields per layer for an N layer laminate). This model belongs to the family of multi-particle models developed in [11–17]. In [14], Hadj-Ahmed et al. used a layerwise model to analyse the variations on the

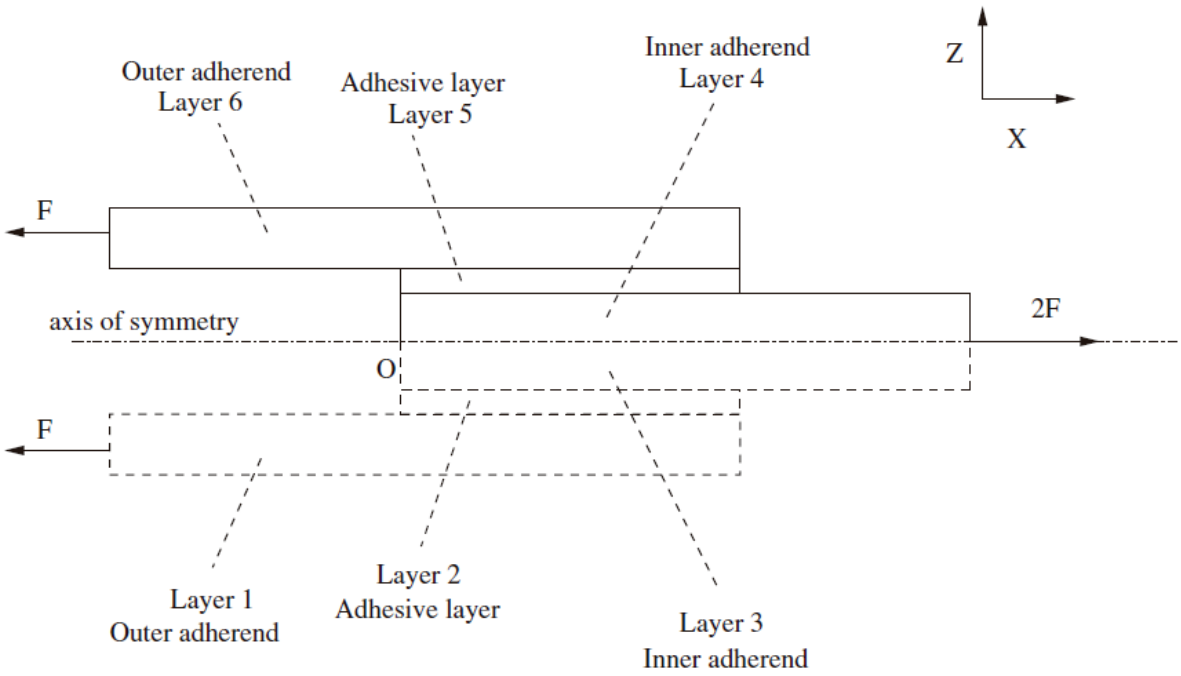

Fig. 1. Symmetrical adhesively bonded double lap joint.

interlaminar shear stresses due to geometry changes in an adhesive joint. Their model provides more accurate interlaminar shear stresses than a shear lag model but it cannot determine the interlaminar normal stresses. The M4-5N is more complex than the previous model and is similar to Pagano's local model [18]. By applying this model, the multi-layer is modelled by a stacking of Reissner plates [19] (one plate for each layer) coupled by inter- laminar stresses (shear and normal stresses). Its equations are obtained by adapting the Hellinger–Reissner varia- tional formulation [20]. For its validation, the following consideration was taken into account: the results of finite element analysis represent the standard to which all other results are compared, and when a new method of analysis yields similar results to those of finite element analysis, the new method is considered adequate. The comparison between the model

results and those of solid finite elements performed by Carreira et al. validated the model for free edge problems [17]. The main advantages of using the M4-5N model rather than solid finite elements is the enormous difference in computational cost and the lack of stress singularities at the interfaces. Since the inter- laminar stresses of the model are finite, a maximum stress criterion has been proposed to predict delamination onset in [16,21] for free edge delamination tests with carbon- epoxy laminates. The model predictions proved to be very accurate.

In the present paper, the M4-5N equations are applied to evaluate the stress state in an adhesively bonded joint. The adhesive is considered as a plate rather than an interface as proposed in the shear lag models. The adhesive has then two interfaces in the model. The interlaminar stresses at these interfaces are a priori different. The problem is formulated under the follow-ing simplifying assumptions: (i) the adhesive joint is symmetrical, which significantly reduces the number of primary unknowns in the problem; and (ii) the adhesive joint is in a state of plane strain. The results of the M4-5N model, a shear lag model and a commercial finite ele-ment software are compared in order to prove the accuracy of the M4-5N and its advantages over the other model.

This paper is divided into three sections. The first one shows the model equations applied to the mechanical problem of a double-lap adhesively bonded joint. In the second section, a differential equation set is obtained and is solved by means of a variational formulation. In the last section, the results of the M4-

5N model are compared with those of a 3D finite element calculation and a shear lag model [1]. In this comparison, only the interlaminar stresses at the adhesive–adherend interfaces are considered.

The three-dimensional object studied in this work is a symmetrical, double lap adhesive joint (the number of layers is n ¼ 6; see Fig. 1).

The layers are numbered from 1 to 6 from the bottom to the top. Layers 1 and 6 are the outer adherends, and layers 3 and 4 constitute the inner adherend. The 2nd and the 5th layers serve to model the adhesive. The lay up direction is z and the tensile force F is applied in the x-direction. The overlap length is l. In each layer i, h_i^-, h_i^+ and $\overline{h_i}$ are the bottom, the top and the mid-plane z coordinates $(h_{i+1}^- = h_i^+)$, respectively. The thickness of layer i is the bottom, the top and the mid-plane z coordinates $(h_{i+1}^- = h_i^+)$ respectively. The thickness of layer i is then $e^i = h_i^+ - h_i^-$. In this section, the equations of the M4-5N model are applied to this problem and very few demonstra-tions of the model equations are provided since all the details of the construction of the model can be found in [12,16,17].

The first step in building the model is the approximation of the stress field $\boldsymbol{\sigma}(x,z)$ in each layer by means of z-polynomials [12,17]. The y coordinate and vector components on the y-direction do not appear in any of the equations because of the plane strain hypothesis, except for $\sigma_{22}(x,z)$. For the components $\sigma_{11}(x,z)$ and $\sigma_{22}(x,z)$ of the stress field in layer i, two first degree z-polynomials are chosen. The degree of the polynomial approximation of the other stress components are deduced

from the three dimensional equilibrium equations:

$$\begin{cases} \dfrac{\partial \sigma_{11}(x,z)}{\partial x} + \dfrac{\partial \sigma_{13}(x,z)}{\partial z} = 0, \\ \dfrac{\partial \sigma_{22}(x,z)}{\partial y} = 0, \\ \dfrac{\partial \sigma_{13}(x,z)}{\partial x} + \dfrac{\partial \sigma_{33}(x,z)}{\partial z} = 0. \end{cases} \tag{1}$$

Let us remark that the second equation is automatically verified.

In this manner, in each layer i the degree of the $\sigma_{13}(x,z)$ and $\sigma_{33}(x,z)$ polynomials are 2 and 3, respectively. The polynomial approximation of the stress field in layer i is then

$$\begin{cases} \sigma_{11}(x,z) = a^i_{11}(x)P^i_0(z) + b^i_{11}(x)P^i_1(z), \\ \sigma_{13}(x,z) = a^i_{13}(x)P^i_0(z) + b^i_{13}(x)P^i_1(z) \\ \qquad\qquad + c^i_{13}(x)P^i_2(z), \\ \sigma_{22}(x,z) = a^i_{22}(x)P^i_0(z) + b^i_{22}(x)P^i_1(z), \\ \sigma_{33}(x,z) = a^i_{33}(x)P^i_0(z) + b^i_{33}(x)P^i_1(z) \\ \qquad\qquad + c^i_{33}(x)P^i_2(z) + d^i_{33}(x)P^i_3(z), \end{cases} \tag{2}$$

where the family $P^i_j\ (0 \leqslant j \leqslant 3)$ is a basis of third-degree z-polynomials:

$$
\begin{cases}
P_0^i(z) = 1, \\
P_1^i(z) = \dfrac{z - \overline{h}_i}{e^i}, \\
P_2^i(z) = -6\left(\dfrac{z - \overline{h}_i}{e^i}\right)^2 + \dfrac{1}{2}, \\
P_3^i(x, z) = -2\left(\dfrac{z - \overline{h}_i}{e^i}\right)^3 + \dfrac{3}{10}\left(\dfrac{z - \overline{h}_i}{e^i}\right).
\end{cases}
$$

The coefficients of these polynomials that appear in Eq. (2) are

$$
\begin{cases}
a_{11}^{i}(x) = \dfrac{N_{11}^{i}(x)}{e^{i}}, \\
b_{11}^{i}(x) = \dfrac{12M_{11}^{i}(x)}{(e^{i})^{2}}, \\
a_{13}^{i}(x) = \dfrac{Q_{1}^{i}(x)}{e^{i}}, \\
b_{13}^{i}(x) = \tau^{i,i+1}(x) - \tau^{i-1,i}(x), \\
c_{13}^{i}(x) = \dfrac{Q_{1}^{i}(x)}{e^{i}} - \dfrac{\tau^{i,i+1}(x) + \tau^{i-1,i}(x)}{2}, \\
a_{22}^{i}(x) = \dfrac{N_{22}^{i}(x)}{e^{i}}, \\
b_{22}^{i}(x) = \dfrac{12M_{22}^{i}(x)}{(e^{i})^{2}}, \\
a_{33}^{i}(x) = \dfrac{v^{i,i+1}(x) + v^{i-1,i}(x)}{2} \\
\qquad + \dfrac{e^{i}}{12}\dfrac{\mathrm{d}}{\mathrm{d}x}(\tau^{i,i+1}(x) - \tau^{i-1,i}(x)), \\
b_{33}^{i}(x) = -\dfrac{\mathrm{d}}{\mathrm{d}x}\dfrac{Q_{1}^{i}(x)}{5} + \dfrac{e^{i}}{10}\dfrac{\mathrm{d}}{\mathrm{d}x}(\tau^{i,i+1}(x) + \tau^{i-1,i}(x)) \\
\qquad + v^{i,i+1}(x) - v^{i-1,i}(x), \\
c_{33}^{i}(x) = \dfrac{e^{i}}{12}\dfrac{\mathrm{d}}{\mathrm{d}x}(\tau^{i,i+1}(x) - \tau^{i-1,i}(x)), \\
d_{33}^{i}(x) = -\dfrac{\mathrm{d}Q_{1}^{i}(x)}{\mathrm{d}x} + \dfrac{e^{i}}{2}\dfrac{\mathrm{d}}{\mathrm{d}x}(\tau^{i,i+1}(x) + \tau^{i-1,i}(x))
\end{cases}
\tag{4}
$$

and are related to the following generalized internal forces:

membranar forces in layer i:

$$N_{11}^{i}(x) = \int_{h_i^-}^{h_i^+} \sigma_{11}(x,z)\,\mathrm{d}z$$

and

$$N_{22}^{i}(x) = \int_{h_i^-}^{h_i^+} \sigma_{22}(x,z)\,\mathrm{d}z \tag{5}$$

bending moment in layer i:

$$M_{11}^{i}(x) = \int_{h_i^-}^{h_i^+} (z-\overline{h}_i)\sigma_{11}(x,z)\,\mathrm{d}z$$

and

$$M_{22}^{i}(x) = \int_{h_i^-}^{h_i^+} (z-\overline{h}_i)\sigma_{22}(x,z)\,\mathrm{d}z \tag{6}$$

vertical shear force in layer i:

$$Q_{1}^{i}(x) = \int_{h_i^-}^{h_i^+} \sigma_{13}(x,z)\,\mathrm{d}z \tag{7}$$

interlaminar shear stress at interface $^{i,\,i+1}$:

$$\tau^{i,i+1}(x) = \sigma_{13}(x,h_i^+) \tag{8}$$

and interlaminar normal stress at interface

$$v^{i,i+1}(x) = \sigma_{33}(x,h_i^+). \tag{9}$$

By introducing the polynomial approximation into Eq. (1), one obtains the

generalized equilibrium equations for each layer $i\ (1 \leqslant i \leqslant 6)$:

$$N_{11}^{i\prime}(x) + \tau^{i,i+1}(x) - \tau^{i-1,i}(x) = 0, \tag{10}$$

$$M_{11}^{i\prime}(x) - Q_1^i(x) + \frac{e^i}{2}(\tau^{i,i+1}(x) + \tau^{i-1,i}(x)) = 0, \tag{11}$$

$$Q_1^{i\prime}(x) + \nu^{i,i+1}(x) - \nu^{i-1,i}(x) = 0, \tag{12}$$

where $\tau^{0,1} = \nu^{0,1} = \tau^{6,7} = \nu^{6,7} = 0.$

Generalized displacements and strains

The generalized displacements associated with the equilibrium conditions in Eqs. (10)–(12) are [12,17]:

the membranar displacement of layer i, denoted by

$$u_1^i(x) = \int_{h_i^-}^{h_i^+} \frac{P_0^i(z)}{e^i} U_1(x,z)\,\mathrm{d}z, \quad i \in [1,n], \tag{13}$$

where U1 is the component of the 3D displacement in the x-direction.

the rotation fi1ðxÞ of layer i:

$$\phi_1^i(x) = \int_{h_i^-}^{h_i^+} \frac{12}{e^{i2}} P_1^i(z) U_1(x,z)\,\mathrm{d}z, \quad i \in [1,n] \tag{14}$$

the out-of-plane displacement $u_3^i(x)$ of layer i:

$$u_3^i(x) = \int_{h_i^-}^{h_i^+} \frac{P_0^i(z)}{e^i} U_3(x,z)\,\mathrm{d}z, \quad i \in [1,n], \tag{15}$$

where *U*3 is the component of the 3D displacement in the z-direction. The generalized strains of the model are deduced from the generalized displacements and are related to the generalized internal forces as follows:

$$\begin{cases} \varepsilon_{11}^{i}(x) = u_1^{i\prime}(x) \longleftrightarrow N_{11}^{i}(x), \\ \chi_{11}^{i}(x) = \phi_1^{i\prime}(x) \longleftrightarrow M_{11}^{i}(x), \\ d_Q^{i}(x) = \phi_1^{i}(x) + u_3^{i\prime}(x) \longleftrightarrow Q_{11}^{i}(x), \\ D^{jj+1}(x) = u_1^{j+1}(x) - u_1^{j}(x) \\ \qquad -\dfrac{e^{j}}{2}\phi_1^{j}(x) - \dfrac{e^{j+1}}{2}\phi_1^{j+1}(x) \longleftrightarrow \tau^{jj+1}(x), \\ D_v^{jj+1}(x) = u_3^{j+1}(x) - u_3^{j}(x) \longleftrightarrow v^{jj+1}(x), \end{cases} \tag{16}$$

where and $1 \leqslant i \leqslant 6$ and $1 \leqslant j \leqslant 5.$

Generalized constitutive equations

The constitutive equations are [12,17]:

membranar behavior of layer *i* (1⩽i⩽6):

$$\begin{pmatrix} \varepsilon_{11}^{i} \\ 0 \end{pmatrix} = \frac{1}{e^{i}} \begin{matrix} S_{1111}^{i} & S_{1122}^{i} \\ S_{1122}^{i} & S_{2222}^{i} \end{matrix} \cdot \begin{pmatrix} N_{11}^{i} \\ N_{22}^{i} \end{pmatrix} \tag{17}$$

in-plane bending behavior of layer *i* (1⩽i⩽6):

$$\begin{pmatrix} \chi_{11}^{i} \\ 0 \end{pmatrix} = \frac{12}{e^{i}} \begin{matrix} S_{1111}^{i} & S_{1122}^{i} \\ S_{1122}^{i} & S_{2222}^{i} \end{matrix} \cdot \begin{pmatrix} M_{11}^{i} \\ M_{22}^{i} \end{pmatrix} \tag{18}$$

out of-plane shear behavior of layer *i* (1⩽i⩽6):

$$d_Q^i(x) = \frac{24S_{1313}^i}{5e^i} Q_1^i(x) - \frac{2S_{1313}^i}{5}(\tau^{i,i+1}(x) + \tau^{i-1,i}(x)) \tag{19}$$

shear behavior of interface i,i+1 (1⩽i⩽5):

$$\begin{aligned} D^{i,i+1}(x) = & -\frac{2S_{1313}^i}{5} Q_1^i(x) - \frac{2S_{1313}^{i+1}}{5} Q_1^{i+1}(x) \\ & - \frac{2S_{1313}^i}{15} \tau^{i-1,i}(x) + \frac{8}{15}(e^i S_{1313}^i \\ & + e^{i+1} S_{1313}^{i+1}) \tau^{i,i+1}(x) - \frac{2S_{1313}^{i+1}}{15} \tau^{i+1,i+2}(x) \end{aligned} \tag{20}$$

and peeling behavior of interface i,i+1 (1⩽i⩽5):

$$\begin{aligned} D_v^{i,i+1}(x) = & \frac{9S_{3333}^i}{70} e^i v^{i-1,i} \\ & + \frac{13}{35}(e^i S_{3333}^i + e^{i+1} S_{3333}^{i+1}) v^{i,i+1}(x) \\ & + \frac{9}{70} e^{i+1} S_{3333}^{i+1} v^{i+1,i+2}(x), \end{aligned} \tag{21}$$

where $S_{opqr}^i \ ((o,p,q,r) \in \{1,2,3\}^4)$ are the components of the fourth order compliance tensor, $\tau^{0,1} = v^{0,1} = \tau^{6,7} = v^{6,7} = 0.$. Let us point out that in the proposed model, the interfaces of the joint are coupled by the interlaminar constitutive equations.

2.4. Generalized boundary conditions

Let us now determine the boundary conditions of the problem. First, the geometry of the problem is reduced in order to apply easily the model equations

(see Fig. 2). This geometry simplification requires an additional analysis for the selection of the pertinent boundary conditions to the new geometry.

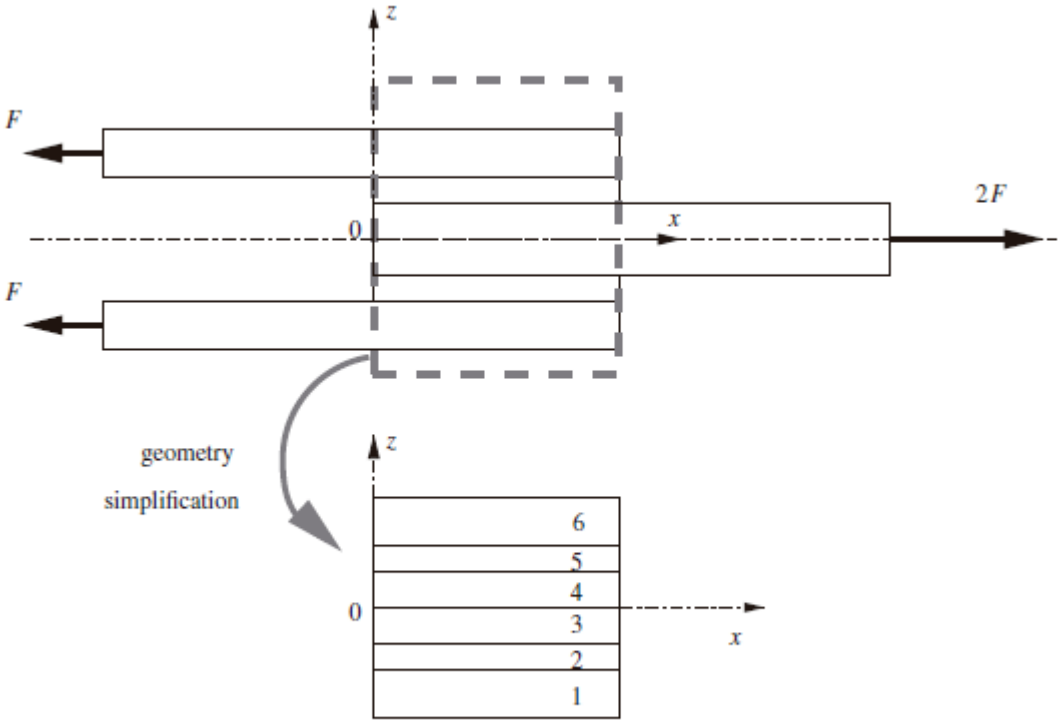

Fig. 2. First geometry simplification.

Generalized boundary conditions

Let us now determine the boundary conditions of the problem. First, the geometry of the problem is reduced in order to apply easily the model equations (see Fig. 2). This geometry simplification requires an additional analysis for the selection of the pertinent boundary conditions to the new geometry.

At the edges of the multilayer, the following boundary conditions [12,17] must be satisfied

$$\begin{cases} N_{11}^{i}(0) = -\int_{h_i^-}^{h_i^+} T_1^l \, \mathrm{d}z, \\ M_{11}^{i}(0) = -\int_{h_i^-}^{h_i^+} T_1^l (z - \overline{h}_i) \, \mathrm{d}z, \\ Q_1^{i}(0) = -\int_{h_i^-}^{h_i^+} T_3^l \, \mathrm{d}z \end{cases}$$

and

$$\begin{cases} N_{11}^{i}(l) = \int_{h_i^-}^{h_i^+} T_1^r \, \mathrm{d}z, \\ M_{11}^{i}(l) = \int_{h_i^-}^{h_i^+} T_1^r (z - \overline{h}_i) \, \mathrm{d}z, \\ Q_1^{i}(l) = \int_{h_i^-}^{h_i^+} T_3^r \, \mathrm{d}z, \end{cases} \tag{22}$$

where T1l, T3l, T1r and T3r are the components of the external surface forces applied at the edges of the multilayer, superscripts *l* and *r* refer to the left and right edges, respectively. At the left edge (x=0), layers 2–5 are stress-free but layers 1 and 6 are subjected to a mechanical load which must be expressed in terms of generalized fields:

the selection of the values of N11i(0) and Q1i(0) is obvious:

$$N_{11}^{1}(0) = \frac{F}{b}, \quad N_{11}^{6}(0) = \frac{F}{b},$$

$$Q_1^{1}(0) = 0 \quad \text{and} \quad Q_1^{6}(0) = 0,$$

where *b* is the width of the joint;

the selection of the correct value of M11i(0) is not so simple. For simplicity sake, the bending moment in layers 1 and 6 is neglected.

At the right edge (x=l), layers 1,2,5 and 6 are stress-free but layers 3 and 4 are subjected to a mechanical load which must be expressed in terms of generalized

fields:

the selection of the values of N11i(l) and Q1i(l) is obvious:

$$N_{11}^{3}(l)=\frac{F}{b},\quad N_{11}^{4}(l)=\frac{F}{b},$$

$$Q_{1}^{3}(l)=0\quad\text{and}\quad Q_{1}^{4}(l)=0$$

due to the symmetry at the z=0 plane, it is better to chose zero rotations instead of bending moments.

In short, the boundary conditions are

$$\begin{cases} N_{11}^{1}(0)=\dfrac{F}{b}, \\ N_{11}^{6}(0)=\dfrac{F}{b}, \\ N_{11}^{i}(0)=0 \quad \text{for } 2\leqslant i\leqslant 5, \\ Q_{1}^{i}(0)=0 \quad \text{for } 1\leqslant i\leqslant 6, \\ M_{11}^{i}(0)=0 \quad \text{for } 1\leqslant i\leqslant 6 \end{cases}$$

and

$$\begin{cases} N_{11}^{i}(l)=0 \quad \text{for } i\in\{1,2,5,6\}, \\ N_{11}^{i}(l)=\dfrac{F}{b} \quad \text{for } i\in\{3,4\}, \\ Q_{1}^{i}(l)=0 \quad \text{for } 1\leqslant i\leqslant 6, \\ M_{11}^{i}(l)=0 \quad \text{for } i\in\{1,2,5,6\}, \\ \phi_{1}^{i}(l)=0 \quad \text{for } i\in\{3,4\}. \end{cases} \tag{23}$$

3. Resolution of the model equations

The resolution of the model equations is similar to that made by Diaz et al. in [23]. In all, we have introduced 86 unknown fields:

$$\begin{cases} N_{11}^{i}, N_{22}^{i}, Q_{1}^{i}, M_{11}^{i}, M_{22}^{i}, \tau^{j,j+1}, \nu^{j,j+1}, \\ u_{1}^{j}, u_{3}^{j}, \phi_{1}^{i}, \varepsilon_{11}^{i}, \chi_{11}^{i}, d_{Q}^{i}, D^{j,j+1}, D_{v}^{j,j+1} \end{cases}$$

$$\text{for} \begin{cases} 1\leqslant i\leqslant 6 \\ 1\leqslant j\leqslant 5 \end{cases} \tag{24}$$

and 86 equations (18 equilibrium conditions in Eqs. (10)–(12), 28 equations that relate the generalized strains to the generalized displacements in Eq. (16), and 40 constitutive laws in Eqs. (17)–(21)).

To simplify the resolution of the problem equations, we have reduced the number of unknowns by applying the symmetry with respect to the z=0 plane. By making use of this symmetry and replacing the generalized strains in Eqs. (17)–(21) by their expressions in Eq. (16), we obtain 29 unknowns:

$$\begin{cases} N_{11}^i, N_{22}^i, Q_1^i, M_{11}^i, M_{22}^i, \tau^{i,i+1}, v^{i,i+1}, \\ u_1^i, u_3^i, \phi_1^i \end{cases} \quad \text{for} \begin{cases} 1 \leqslant i \leqslant 3, \\ 1 \leqslant j \leqslant 2. \end{cases} \tag{25}$$

Let us remark that τ3,4 is zero and therefore it is not considered as an unknown of the problem. The 29 equations that help to determine these unknowns are

- Eqs. (10)–(12) for $1 \leqslant i \leqslant 3$.
- Eqs. (17)–(21) for $1 \leqslant i \leqslant 3$.
- Eq. (20) for $1 \leqslant i \leqslant 2$.

Let us define an eight size vector γ which components are

$$\gamma_i = Q_1^i, \quad \gamma_{3+j} = u_1^{j+1} - u_1^j, \quad \gamma_{5+i} = \phi_1^i, \tag{26}$$

where 1⩽i⩽3 and 1⩽j⩽2. A last simplification of the problem can be obtained by expressing the 29 unknowns in Eq. (25) as linear functions of the components of vector γ. This is performed by following the steps detailed in Appendix B. Using these steps, the following set of eight second-order differential equations is obtained [23]:

(27)γ″(x)=M·γ(x),

where M is a constant (8×8) size matrix. The coefficients of this matrix are functions of the mechanical and geometrical characteristics of the adhesive joint.

The resolution of the differential equation set (27) requires 2×8 boundary conditions that are deduced from the boundary conditions in Eq. (23)

$$\begin{cases} \gamma_i(0) = 0, \\ \gamma'_4(0) = -\dfrac{S^1_{1111}}{e^1} \times F, \\ \gamma'_5(0) = 0, \\ \gamma'_{5+i}(0) = 0 \end{cases}$$

and

$$\begin{cases} \gamma_i(l) = 0, \\ \gamma'_4(l) = 0, \\ \gamma'_5(l) = \dfrac{S^3_{1111}}{e^3} \times F, \quad \text{for } 1 \leqslant i \leqslant 3. \\ \gamma'_6(l) = \gamma'_7(l) = 0, \\ \gamma_8(l) = 0 \end{cases} \tag{28}$$

In order to solve the differential equation set in Eq. (27). The [0,l] interval is divided into *N* subintervals [ap,ap+1] (0⩽p⩽N). In each subinterval, the components of γ are approximated by linear *x*-functions. Eq. (27) and a varational formulation lead to resolving the following set of 8×(N-1) linear algebraic equations:

$$\boldsymbol{R} \cdot \boldsymbol{\xi} = \boldsymbol{c}, \tag{29}$$

where R is an 8(N-1)×8(N-1) size constant matrix, c an 8(N-1) size constant vector

and ξ an 8(N-1) size unknown vector. The components of ξ are the values of the γ components at discrete points ap. The system stiffness matrix R is a sparsely populated matrix and is stored by means of the skyline storage scheme [24]. This technique allows a considerable saving in storage.

The equilibrium and constitutive equations provide the nodal values of the remaining unknown model fields.

4. Applications

In this section, we compare the results of our model with those of a shear lag model and a finite element calculation by means of the software SAMCEF (SAMTECH, Liege, Belgium). For the comparison with the shear lag model, we only compare the shear stresses in the adhesive layer. In the adhesive, the shear lag model yields a mean shear stress τ(x) expressed by

$$\tau(x) = \frac{F}{b}\frac{G_{13}^2}{e^2\lambda}\left[\left(\frac{1}{e^1E_{11}^1\tanh(\lambda l)} + \frac{1}{e^3E_{11}^3\sinh(\lambda l)}\right)\cosh(\lambda x) - \frac{1}{e^1E_{11}^1}\sinh(\lambda x)\right], \quad (30)$$

where

$$\lambda = \frac{G_{13}^2}{e^2}\left(\frac{1}{e^1E_{11}^1} + \frac{1}{e^3E_{11}^3}\right).$$

where

$$\lambda = \frac{G_{13}^2}{e^2}\left(\frac{1}{e^1E_{11}^1} + \frac{1}{e^3E_{11}^3}\right).$$

The determination of this analytical solution is provided in Appendix A. For the numerical applications, we consider two types of joints: a homogeneous joint (same mechanical characteristics for adherends 1 and 3) and a heterogeneous joint

(different mechanical characteristics for adherends 1 and 3). The mechanical properties required to calculate the shear stress by means of Eq. (30) are shown in Tables 1 and 2 for the homogeneous and heterogeneous joints, respectively. For both joints, the overlap legth is l=40mm, the width is b=10mm, and the applied force is F=5000N. Our comparisons between the different calculation techniques applied to these joints focus on the values of the shear and normal stresses in the adhesive.

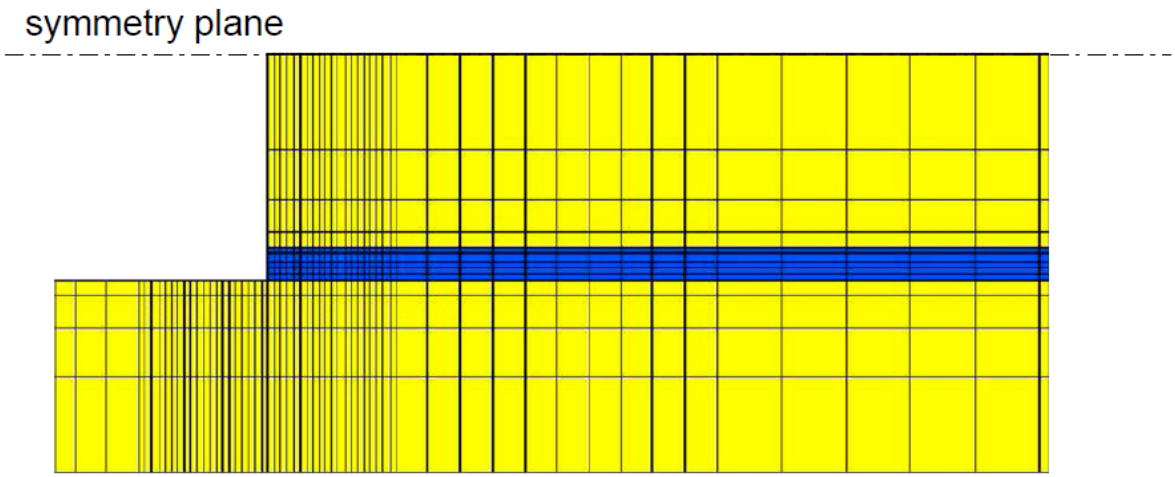

Fig. 3. Mesh of half of the symmetrical, double lap adhesive joint.

For our M4-5N model calculations, we used an 80-node mesh along the bond length. The node density was greater at the ends of the bond.

Comparison of the interlaminar shear stresses

Homogeneous adhesive joint

According to Goland and Reissner [2], a shear lag model is valid whenever Gec/Gce⩾10; where r,G and Gc are the shear moduli of the adherend and adhesive, respectively, and *e* and ec are the corresponding thicknesses. In this case we can assume that the adhesive is subjected mostly to shear stresses, whereas the adherends are subjected mostly to tensile stresses. In our application example the

ratio Gec/Gce is 8.7. This means that the Goland and Reissner condition is not verified but since this value is close to 10, one may think that the shear lag model could provide a fairly good approximation of the stress field.

Figs. 4 and 5 reveal that the shear lag model provides the same solution at interfaces 1,2 and 2,3 and slightly overestimates the maximum shear stress values predicted by the finite element calculations. In addition, these maxima are reached exactly at the bond ends. Our M4-5N model provides a very accurate and better approximation of the interlaminar shear stresses. Besides, our model and SAMCEF reach the maxima at almost the same places. We can note herein that even if the joint is symmetrical $(\text{i.e. } e^1 = e^3)$ and balanced $(\text{i.e. } e^1 E_{11}^1 = e^3 E_{11}^3)$, our model and SAMCEF provide both different maximum values of the shear stress at the left and at the right ends of the adhesive.

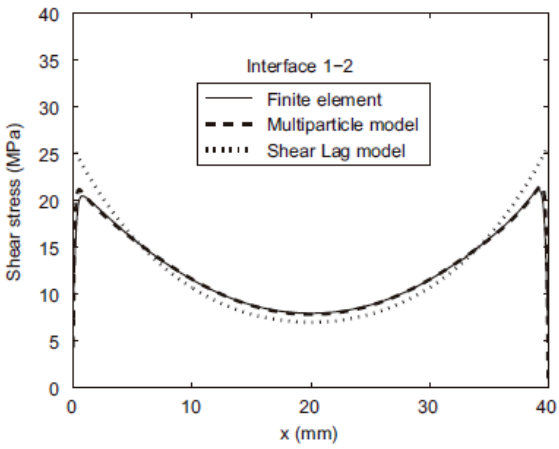

Fig. 4. Interlaminar shear stress $\tau^{1,2}$ in a homogeneous adhesive joint.

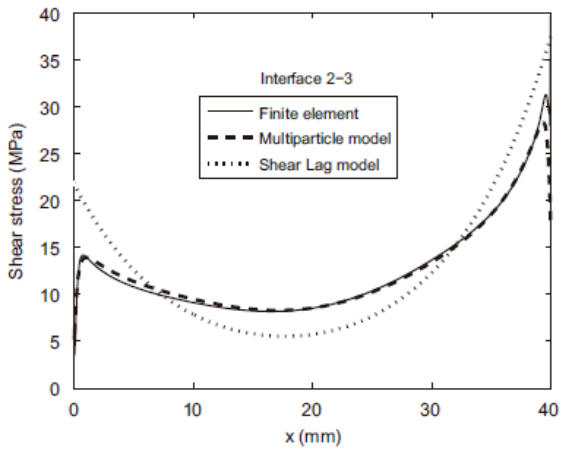

Fig. 7. Interlaminar shear stress $\tau^{2,3}$ in a heterogeneous adhesive joint.

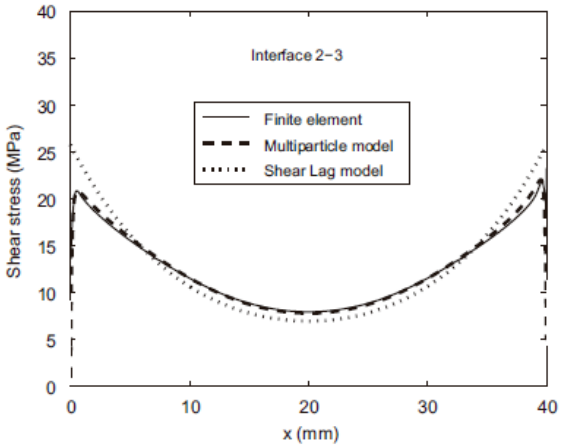

Fig. 5. Interlaminar shear stress $\tau^{2,3}$ in a homogeneous adhesive joint.

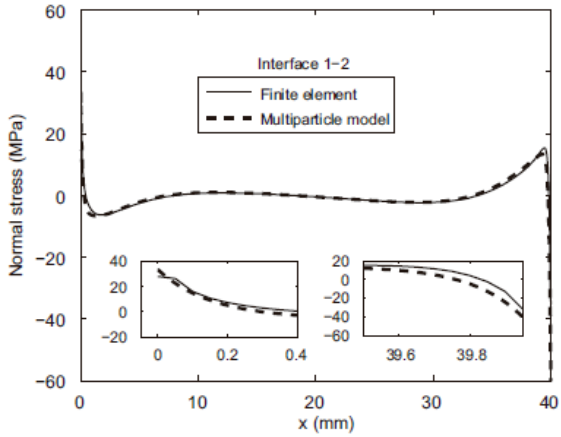

Fig. 8. Interlaminar normal stress $\nu^{1,2}$ in a heterogeneous adhesive joint.

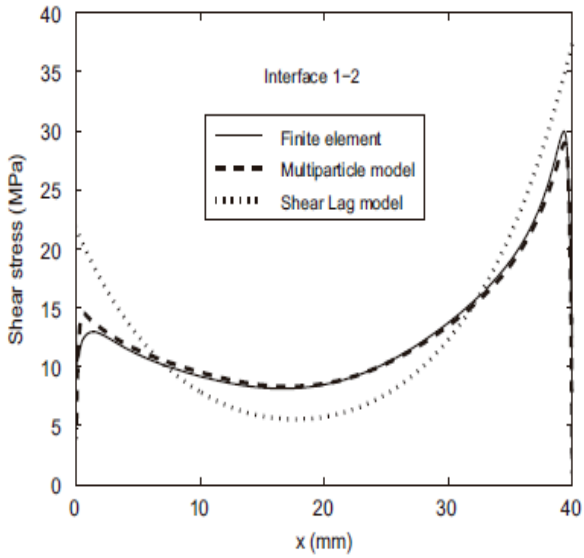

Fig. 6. Interlaminar shear stress $\tau^{1,2}$ in a heterogeneous adhesive joint.

The ratio Gec/Gce is now 0.5. We remark in Figs. 6 and 7 that the difference between the shear lag solution and the finite element calculation is quite significant. On the contrary, our M4-5N model gives once again an accurate prediction. It should be pointed out that for this joint, the maximum values of the shear stress at the two ends are very different.

Comparison of the interlaminar normal stresses

We are only interested herein in a heterogeneous adhesive joint. The stresses resulting from a finite element calculation are often singular, i.e. the maximum stress value depends on the level of mesh refinement. In order to make a comparison between the finite element calculation and our model, the meshing is refined in such a way that the stress singularity is not very significant. Let us recall that our mesh has five rows of elements in the adhesive layer.

Figs. 8 and 9 display the normal stress at interfaces 1,2 and 2,3, respectively. We can observe that the normal stress is zero on nearly the entire overlap. Normal stress concentrations are confined to a very small distance from the bond ends. In our model, the maximum values are reached at exactly the end of the bond. The model results converge and do not exhibit any singularity [17,23].

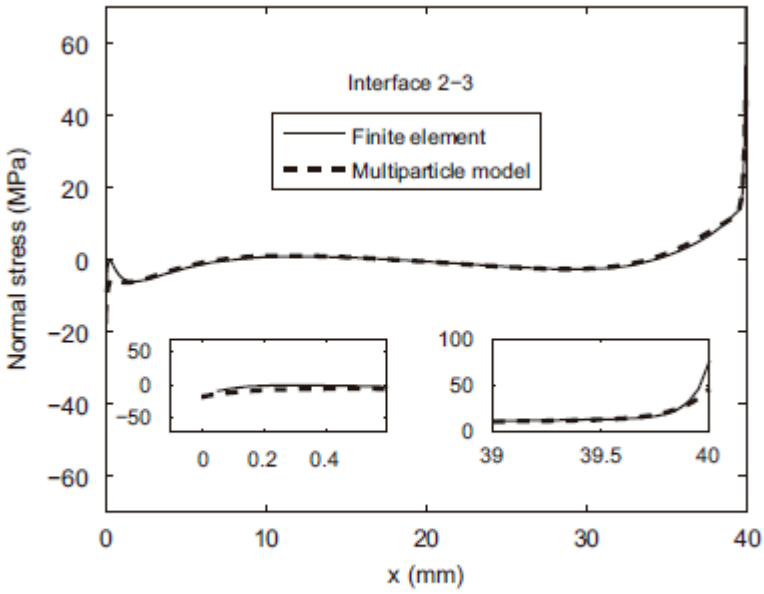

Fig. 9. Interlaminar normal stress $\nu^{2,3}$ in a heterogeneous adhesive joint.

Adams and Wake [6] showed that even if the joint is symmetrical, external adherends bend in the vicinity of the bond edges. The bending moments involve a high normal compressive stress at the left edge (x=0) and wrenching at the right edge (x=l). For a single lap adhesive joint, these interlaminar normal stresses are very significant. The normal and shear stresses calculated by our model and SAMCEF are similar. Moreover, for our model, at each edge the maximum values of normal stresses at interfaces 1,2 and 2,3 are different.

5. Conclusion

In this paper, we have proposed a layerwise model for calculating the interlaminar stresses in a symmetrical, double lap adhesively bonded joint. The model equations were solved by means of a finite element technique. For its validation, we have compared its results to those of a solid finite element analysis: the standard method by which correctness of other methods is judged.

Through the use of two examples, we have shown that our model yields an accurate prediction of the maximum values of both the interlaminar shear and normal stresses, particularly when the joint does not satisfy the Goland and Reissner condition. In this case, we have shown that a shear lag model does not predict correctly the maximum stress values. Furthermore, as opposed to finite element calculations, our model provides finite maximum values of the interlaminar stresses. In this manner, our model and a maximum stress criterion may predict the joint failure and this prediction may be as accurate as those proposed in [21,22] for carbon-epoxy laminates subjected to a tensile load. Other advantages of our model over classical finite element calculations are the reduced computation time and ease of calculation. In a subsequent paper, several mechanical tests will be performed in order to determine a failure criterion for adhesively bonded joints by means of the model shown in the present paper.

Appendix A. Longitudinal shear stress in the adhesive layer (shear lag model)

For an adhesive joint, a shear lag model assumes that the shear stress in the adhesive is proportional to the difference between the displacements of the outer adherend (layer 1) u1(x) and the inner adherend (layer 3) u3(x):

$$\tau(x) = \frac{G_c}{e}(u^3(x) - u^1(x)). \quad \text{(A.1)}$$

The elastic behavior of the adherends leads to:

$$\begin{cases} \dfrac{\mathrm{d}u^1(x)}{\mathrm{d}x} = \dfrac{\sigma^1(x)}{E^1}, \\ \dfrac{\mathrm{d}u^3(x)}{\mathrm{d}x} = \dfrac{\sigma^3(x)}{E^3}. \end{cases} \tag{A.2}$$

Thus, Eq. (A.1) becomes

$$\frac{\mathrm{d}\tau(x)}{\mathrm{d}x} = \frac{G_c}{e}\left(\frac{\sigma^3(x)}{E^3} - \frac{\sigma^1(x)}{E^1}\right), \tag{A.3}$$

where σ1(x) and σ3(x) are the tensile stresses in adherends 1 and 3, respectively; E1 and E3 are the elastic moduli of adherends 1 and 3, respectively.

The equilibrium equations are

$$\begin{cases} e^1\dfrac{\mathrm{d}\sigma^1(x)}{\mathrm{d}x} = -\tau(x), \\ e^3\dfrac{\mathrm{d}\sigma^3(x)}{\mathrm{d}x} = \tau(x), \end{cases} \tag{A.4}$$

where e1 and e3 are the thicknesses of adherends 1 and 3, respectively. The boundary conditions are

$$\begin{cases} be^1\sigma^1(0) = F, \\ be^3\sigma^3(0) = 0 \end{cases} \quad \text{and} \quad \begin{cases} be^1\sigma^1(l) = 0, \\ be^3\sigma^3(l) = F, \end{cases} \tag{A.5}$$

where *b* is the width of the joint. By eliminating σ1(x) and σ3(x) from Eqs. (A.3) and (A.4), we obtain:

$$\frac{d^2\tau(x)}{\mathrm{d}x^2} = \frac{G_c}{e}\left(\frac{1}{e^1E^1} + \frac{1}{e^3E^3}\right)\tau(x). \tag{A.6}$$

Let us define

$$\lambda = \frac{G_c}{e}\left(\frac{1}{e^1 E^1} + \frac{1}{e^3 E^3}\right).$$

By making use of Eqs. (A.3) and (A.5), the resolution of Eq. (A.6) provides the expression of τ in Eq. (30).

Appendix B. Simplification of the model equations

The components of γ

$$\gamma_i = Q_1^i, \quad \gamma_{3+j} = u_1^{j+1} - u_1^j,$$
$$\gamma_{5+i} = \phi_1^i \quad \text{for } 1 \leqslant i \leqslant 3 \quad \text{and } 1 \leqslant j \leqslant 2 \qquad \text{(B.1)}$$

are called the primary unknowns of the problem. In this section, the steps to follow for writing the 29 unknowns in (25) as linear functions of the primary unknowns are described.

(1)

By using Eq. (20) (written for $1 \leqslant i \leqslant 2$) the vector $(\tau 1,2, \tau 2,3)t$ can be written as the multiplication of a 2×8 constant matrix by the γ vector.

(2)

Eq. (21) (written for $1 \leqslant i \leqslant 3$) shows that the expression of $v_{i,i+1}$ is a linear combination of $u3k$. Furthermore, $u3i'$ is given from Eq. (19) (written for $1 \leqslant i \leqslant 3$) as a linear algebraic (l.a.) equation including the primary unknowns. By deriving $Q1i'$ with respect to *x* in the equilibrium equation (12) (written for $1 \leqslant i \leqslant 3$) and by applying the equations described above in this step, we obtain the expression of $Q1i''$ as an l.a. equation involving the γ components.

(3)

We then write the generalized force $N22i$ as a l.a. function of $N11i$ by means of

the l.a. equation appearing in the second line of relation (17) (written for $1 \leqslant i \leqslant 3$).

(4)

After this step, we can write $u1j+1'-u1j'$ as a linear combination of the forces $N11i$ by means of the first line in Eq. (17) (written for $1 \leqslant i \leqslant 3$).

(5)

By deriving with respect to *x* the expressions of $u1j+1'-u1j'$ obtained from the previous step, we can write $u1j+1''-u1j''$ as a l.a. equation involving the primary unknowns. As a matter of fact, $N11i'$ are l.a. functions of the shear stresses $\tau j,j+1$ (see equilibrium equation (10) written for $1 \leqslant i \leqslant 3$), which were expressed in step 1 as l.a. functions of the γ components.

(6)

We then write the generalized moment $M22i$ as a l.a. function of $M11i$ by means of the l.a. equation appearing in the second line of relation (18) (written for $1 \leqslant i \leqslant 3$).

(7)

After this step, we can write $\chi 11i=\varphi 1i'$ as a l.a. of $M11i$ by means of the first line in Eq. (18) (written for $1 \leqslant i \leqslant 3$). By deriving the expression of $\varphi 1i'$ with respect to *x* and by using the equilibrium equations (11) (written for $1 \leqslant i \leqslant 3$), we obtain the expression of $\varphi 1i''$as a l.a. function involving γ.

Steps 2,5 and 7 yield the differential equation set written in Eq. (27).

[1] Volkersen O. Luftfahrtforschung 1938;15:41–7.

[2] Goland M, Reissner E. J Appl Mech 1944;2:17–27.

[3] Hart-Smith LJ. NASA CR 112236, January 1973.

[4] Delale F, Erdogan F, Aydinoglu MN. J Compos Mater 1981;15:249.

[5] Gustafson PA, Bizard A, Waas A. Int J Solids Struct 2007;44: 5774–95.

[6] Adams RD, Wake WC. Structural adhesive joints in engineering. London: Applied Science Publications; 1984.

[7] Shahin K, Taheri F. Comp Struct 2007;81:511–24.

[8] Vidonne MP. Endommagements et ruptures des interfaces dans les multimate´ riaux. Doctoral dissertation, ENS Cachan, 1995.

[9] Desmorat R. Me´ thode d'analyse de la re´ sistance de zones fortement sollicite´ es. Doctoral dissertation, ENS Cachan, 1996.

[10] Berthelot JM. I J Compos Mater 1997;31:1780–805.

[11] Ehrlacher A, Caron JF, Chabot A, Naciri T. In Compte-Rendus des 9me Journes Nationales sur les Composites. Saint-Etienne, 1994.

[12] Chabot A. Analyse des efforts `a l'interface entre les couches des mate´ riaux composites a` l'aide de mode` les multiparticulaires des mate´ riaux multicouches. Doctoral dissertation, Ecole Nationale des Ponts et Chausse´ es, 1997.

[13] Naciri T, Chabot A, Ehrlacher A. Compos Sci Technol 1998;58: 337–43.

[14] Hadj-Ahmed R, Foret G, Ehrlacher A. Int J Adhes Adhes 2001;21: 297–307.

[15] Limam O, Foret G, Ehrlacher A. Comp Struct 2003;59:467–72.

[16] Diaz Diaz A, Caron JF, Carreira RP. CR Acad Sci 2001;329:873–9.

[17] Carreira RP, Caron JF, Diaz Diaz A. Mech Mater 2002;34:217–30.

[18] Pagano NJ. Int J Solids Struct 1978;19:385–400.

[19] Reissner E. J Appl Mech A 1945:69–77.

[20] Reissner E. J Math Phys 1950;29:90–5.

[21] Caron JF, Carreira RP, Diaz Diaz A. CR Acad Sci 1999;327:1291–6.

[22] Diaz Diaz A, Caron JF. Comp Struct 2006;72:438–45.

[23] Diaz Diaz A, Caron JF, Carreira RP. Comp Struct 2002;58:195–208.

[24] Dhatt G, Touzot G. The finite element method displayed. New York: Wiley; 1984.